Asian Journal of Applied Sciences



Preparation and Characterization of Thin Film TiO₂ Dip Coated on Non-Conductive Substrate Prepared from Tetraethyl Orthotitanate Precursor

A.O. Araoyinbo, M.N. Ahmad Fauzi, S. Sreekantan and A. Aziz School of Materials and Mineral Resources Engineering, Engineering Campus, Universiti Sains Malaysia, 14300 Nibong Tebal, Penang, Malaysia

Abstract: Titanium dioxide (TiO₂) prepared through sol gel process is extensively used as a photocatalyst due to the strong oxidizing power of its holes, high photo stability and redox selectivity. In this present work, the microstructure and crystal structure of TiO₂, obtained by a sol-gel procedure in acid, neutral and base were investigated. The TiO₂ sols were prepared by the hydrolysis and condensation of tetraethyl orthotitanate in ethanol at pH 3, 7 and 10 dip coated on a non conductive substrate (glass). The morphology of the film was examined by SEM, EDX and crystallite structure by X-Ray Diffraction (XRD). The XRD pattern was observed to be sensitive to the heat treatment. At calcination temperature of 300 and 500°C, only anatase phase was observed. As calcination temperature was increased to 700°C, the rutile phase was present for the acid and neutral sol of the TiO₂. The XRD data also showed that the crystallite size of TiO₂ increased significantly as the temperature is increased from 300 to 700°C.

Key words: Coating, crystal growth, hydrolysis, photocatalysis, sol-gel

INTRODUCTION

Nano size materials over the years have attracted growing interest due to their unique structure and properties (Miao *et al.*, 2004). Titanium dioxide (TiO₂) semiconductors has been extensively studied because of its unique properties that makes it an active component in photocatalysis (Fujishima *et al.*, 2000; Asahi *et al.*, 2000), photovoltaics (Adachi *et al.*, 2003), biological coatings (Oh *et al.*, 2005) and photo electrolysis (Fujishima and Honda, 1972).

Titanium dioxide possesses three different crystal structures: rutile (tetragonal), anatase (tetragonal) and brookite (orthorhombic). Among these, the anatase phase is known to exhibit better photocatalytic behavior, whereas rutile is the most stable phase (Mark *et al.*, 1983). Even though the energy band gap (3.23 eV) of the anatase phase is wider than that of the rutile (3.02 eV), recombination of electrons and holes occurs much faster on the surface of the rutile phase (Anderson and Bard, 1995). Since, the photocatalytic activity is mostly confined to the surface of the photocatalytic material, its surface area must be increased to maximize the photocatalytic activity. One way to do this is synthesis of nano-sized TiO₂ particles to increase photocatalytic reaction sites on the surface. Also, the amount of the anatase phase must be maximized because the rutile phase shows less photocatalytic activity (Asahi *et al.*, 2001).

Corresponding Author: Alaba O. Araoyinbo, School of Materials and

Mineral Resources Engineering, Engineering Campus,

Universiti Sains Malaysia, 14300 Nibong Tebal, Penang, Malaysia

Tel: +60 17 4402853

A number of methods have been used to prepare ${\rm TiO_2}$ nanoparticle, such as chemical precipitation (Scolan and Sanchez, 1998), microemulsion (Lal *et al.*, 1998), hydrothermal crystallization (Wu *et al.*, 2002) and sol-gel (Arconada *et al.*, 2009). Sol-gel is one of the most successful techniques for preparing nanosized metallic oxide materials with high photocatalytic activities (Sonawane *et al.*, 2003). By tailoring the chemical structure of primary precursor and carefully controlling the processing variables, nanocrystalline products with very high level of chemical purity can be achieved. A typical sol-gel processing consists of hydrolysis and polycondensation of molecular precursors (Zhang *et al.*, 2007). The titania alkoxides may be hydrolyzed Eq. 1 and polycondensed Eq. 2 and 3 to form titanium oxide gel as follows:

$$\equiv \text{Ti-OR} + \text{H}_2\text{O} \rightarrow \equiv \text{Ti-OH} + \text{ROH}$$
 (1)

$$\equiv \text{Ti-OH} + \equiv \text{Ti-OR} \rightarrow \equiv \text{Ti-O-Ti} \equiv +\text{ROH}$$
 (2)

$$\equiv \text{Ti-OH} + \equiv \text{Ti-OH} \rightarrow \equiv \text{Ti-O-Ti} \equiv + \text{H}_2\text{O}$$
 (3)

The main hydrolyzate is $[Ti (OH)_n (H_2O)_{6n}]^{(4-n)^+}$, of which, the amount of water varies with the relative rates of hydrolysis and polycondensation (Aruna *et al.*, 2000). The structures of the titanium monomers in precursor solutions play a significant role in the condensational process (Sun and Gao, 2002) and the final gel molecular precursor structure formation (Diez *et al.*, 2003). The pH value of the precursor solution is a decisive factor in controlling the final particle size (Sugimoto *et al.*, 2003), shape (Yin *et al.*, 2002), phase (Li *et al.*, 2004) and agglomeration (Sugiyama *et al.*, 2002) due to its influence on the relative rates of hydrolysis and polycondensation.

In this work, we study the effect of pH on the titania phase transformation during a sol-gel process from tetraethyl orthotitanate precursor. We prepared nanocrystalline ${\rm TiO_2}$ thin film by using sol-gel technology at different pH. The influence of temperature and the critical size of phase transformation were also investigated.

MATERIALS AND METHODS

Preparation of the Sol

 ${\rm TiO_2}$ sol was prepared by the partial hydrolysis and polycondensation of tetraethyl orthotitanate with water using ethanol as a solvent and ${\rm HNO_3}$ as a catalyst. For the preparation of the titania sol the following materials were used; tetraethyl orthotitanate $({\rm C_8H_{20}O_4Ti}, 10~{\rm mL})$, nitric acid (${\rm HNO_3}, 1.5~{\rm mL})$, sodium hydroxide (NaOH, 1 M), ethanol (C₂H₅OH, 90 mL). A certain amount of deionized water was added to tetraethyl orthortitanate to form a suspension. An exact amount of ${\rm HNO_3}$ and NaOH were added to the suspension and stirred continuously for 3 h. The ${\rm TiO_2}$ sol obtained was dip coated dried and calcined for 2 h. All the above process was performed at room temperature.

Preparation of Acid (pH 3), Neutral (pH 7) and Base (pH 10) Titania Sols

To prepare the acid (pH 3), neutral (pH 7) and base (pH 10) sol, preliminary titania sol described above was added to water, nitric acid, ethanol and sodium hydroxide to adjust the pH. The different sols were properly mixed, sealed from air and stirred at room temperature for 3 h.

Thin Film Preparation and Coating Process

The substrate used for film deposition was quartz glass. In order to prepare the substrates, they were washed with detergent and oxidant solution composed of H_2SO_4 (96%v/v) and H_2O_2 (29.6%v/v) at 3:1 ratio for 30 min. It should be noted that cleaning by oxidant solution is important for proper adhesion of the films. Furthermore, oxidant solution eliminates interfere ions such as Na^+ and Ca^+ which hinder photocatalytic efficiency (Cernigoj *et al.*, 2006). After washing, all the substrates were rinsed with deionized water. The substrates were then treated with a basic solution of NaOH (5% m/v) in certain time and temperature and after this treatment, the obtained substrates were washed with deionized water and dried. The coating process consists of two steps. In the first step, the substrates were immersed into the TiO_2 sol at room temperature for 1 min withdrawal speed of 100 mm min^{-1} in order for the TiO_2 thin films to adhere to the substrates through dip coating method. Subsequently, films were dried at 100° C for 30 min with six successive immersion cycles. In the second step in order to immobilize TiO_2 layer on the substrates, thin films were calcined in a programmable furnace at 300, 500 and 700°C for 2 h.

Characterization of TiO₂ Thin Film

The crystallite size and crystalline phase of the TiO₂ films was determined using an X-ray diffractometer (Bruker D8 Advance X ray diffractometer with Cu target). All peaks measured by XRD analysis were assigned by comparing with those of JCPDS data (21-1272; 21-1276). The crystal size of the TiO₂ during different states of heat treatment was obtained by the XRD line profile analysis. The morphology of the films surface and thickness of films was observed by scanning electron microscope (Model Supra 35VP) and X-ray energy dispersive spectroscopy (EDX).

RESULTS AND DISCUSSION

The Effect of pH on Surface Morphology

Figure 1a-c show the SEM micrograph of the TiO₂ thin film dip coated on quartz glass substrate in acid, neutral and base sol. It is observed that the surface morphology of the films greatly depends on the type of sol. As it can be see, the film from acid, neutral and base sols consist of agglomerated titania particles which may cause the surface to be non uniform. The grain size increases from about 40-350 nm with increasing pH from acid to base, this can be best explained as the average Milliken charge of hydrogen atoms around the titanium coordinated complexes at low pH is much more than at high pH. The complexes will be separated well because of the repulsive force at low pH and result a slow and discrete disposition of the complexes on the performed nuclei, which leads to small nanocrystallites (Yin *et al.*, 2001). At higher pH values, the titanium- coordinated complexes could not be separated well due to less repulsive force and result in a fast disposition, which lead to the grain size increase.

A cross-sectional morphology of the three different sols, from acid, neutral and base is shown in Fig. 2a-c. It can be seen that the different sol pH also influences the film thickness and adhesion to the substrate. The film thickness and adhesion reduces with increasing pH. The acid sol appears to have a better adhesion to the quartz glass compared with the other sols.

Crystalline Phase Assessment

To be able to assess the formation of crystalline phase in the acid, neutral and base sol calcined at different temperature, the thin films prepared from sols and dip coated on quartz

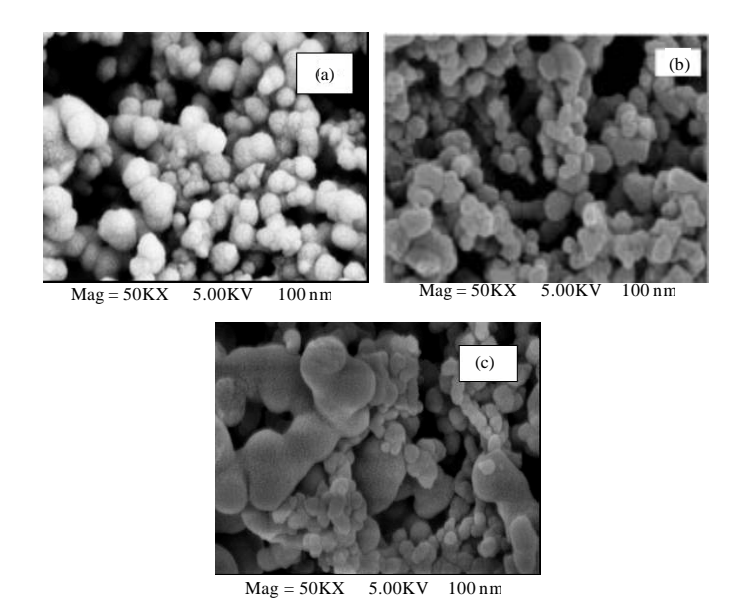


Fig. 1: SEM micrograph of TiO₂ thin film (a) from acid sols, (b) neutral sols and (c) base sols

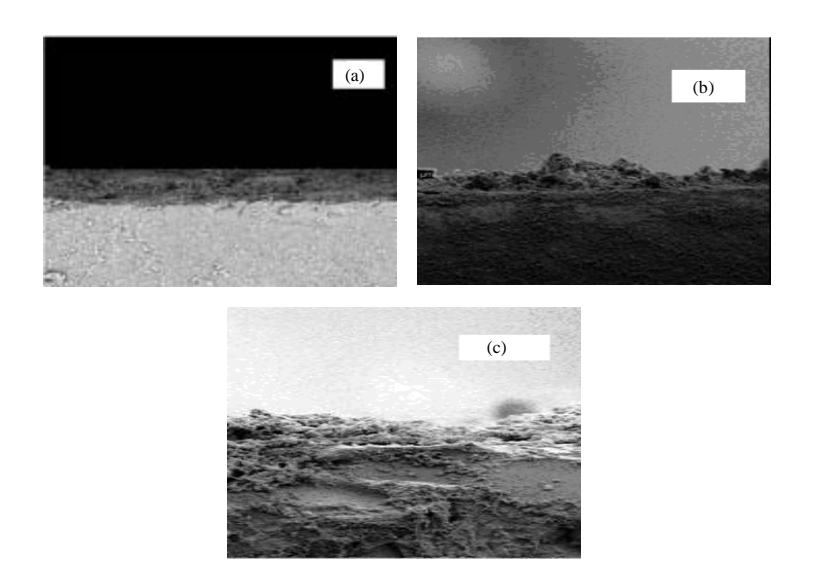


Fig. 2: The cross-sectional morphology of the ${\rm TiO_2}$ thin films (a) dip coated film from acid sols, (b) dip coated film from neutral sols and (c) dip coated film from base sols

glass was analyzed by x-ray diffractometer. The X-ray diffraction patter of TiO_2 thin film at 300, 500 and 700°C is shown in Fig. 3-5. The diffraction patterns indicate a good crystallization of the films prepared by the sol gel procedure. The amorphous phase (not shown) crystallizes to the anatase phase shown in Fig. 3 with peaks at 2 θ of 25.28°, 37.80°, 48.05°, 53.89°, 55.06°, 62.69°, 70.31°, 74.03°, 75.03° and 83.14° are assigned to

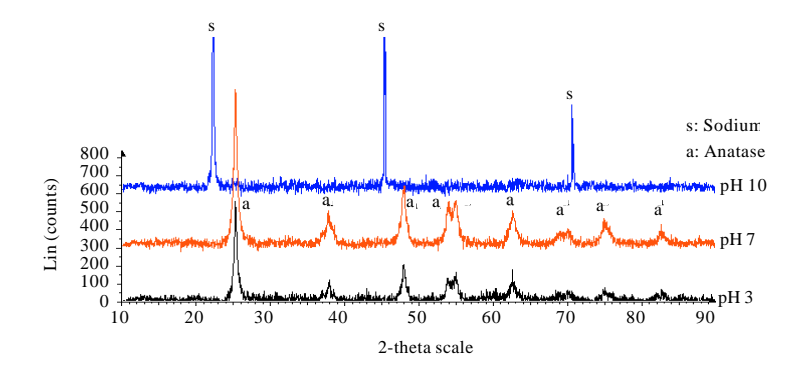


Fig. 3: X-ray diffraction micrograph of TiO₂ thin film at calcination temperature of 300°C

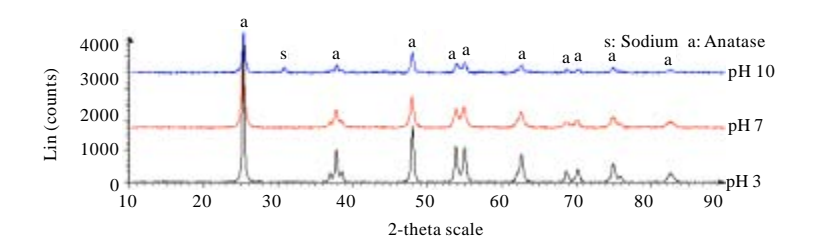


Fig. 4: X-ray diffraction micrograph of TiO₂ thin film at calcination temperature of 500°C

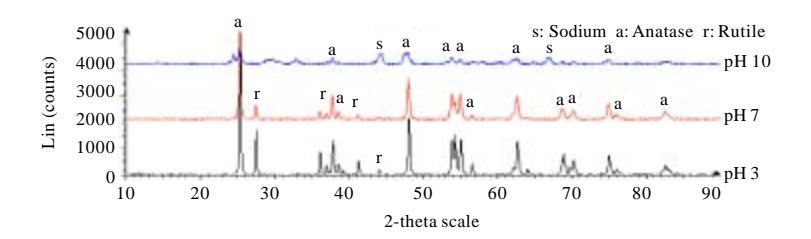


Fig. 5: X-ray diffraction micrograph of TiO₂ thin film at calcination temperature of 700°C

(101), (004), (200), (105), (211), (204), (220), (107), (215) and (312) lattice planes of ${\rm TiO_2}$ at 300°C. At this temperature all the residual organics are believed to be liberated completely. However, the base sol still remains amorphous, this might be as a result sodium Na present suppressing the growth or transformation into the crystallite phase.

As the temperature is increased to 500°C as shown in Fig. 4, the observed predominant phase is till anatase phase with increased intensities at above listed peaks. Figure 5 shows anatase and rutile phases at 700°C to be present in the acid and neutral sol. The rutile phase has its peaks at 2θ of 27.44° , 36.08° , 41.22° and 44.05° are assigned to (110), (101), (111) and (210) lattice planes. The anatase phase maintains its peak positions with further increase in intensities. Only the base sol still predominantly consists of anatase phase with reduced intensities as result of the sodium (Na) present in the sol.

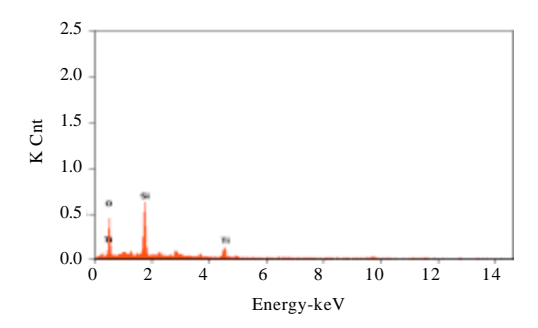


Fig. 6: EDX of TiO₂ thin film prepared from acid sol

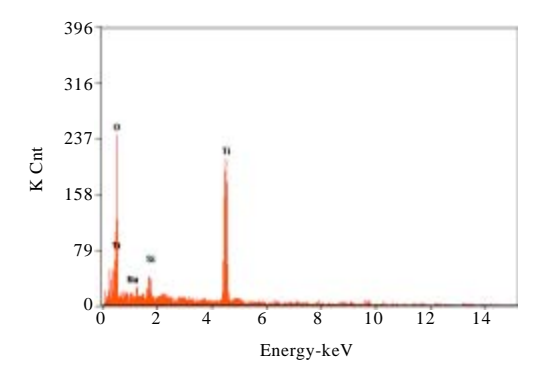


Fig. 7: EDX of TiO₂ thin film prepared from base sol

Figure 6 and 7 show the Energy Dispersive X-ray (EDX) spectrum corresponding to the Ti, O, Na and Si from the substrate. The presence of Na in the base sol accounts for the reason why lower intensities were observed and also the rutile phase not present. The presence of Na is also known to have a negative impact on the photocatalytic capabilities of TiO₂ when exposed to UV-light. The neutral sol also shows the presence of Na but not shown.

Crystallite Size and Weight Fractions Quantification

For crystal size quantification of ${\rm TiO_2}$, the d spacing at 3.52 Å (101) phase for anatase and 3.25 Å (110) phase for rutile were used. X-ray peak-broadening was analyzed by employing the Scherrer equation:

$$L = \kappa \mathcal{N} \beta \cos \theta \tag{4}$$

where, L is the length of the crystal in the direction of the d spacing, κ is a constant of 0.9, λ is the wavelength of the radiation used (1.5405 Å), β is the full width at half-maximum (FWHM) of selected peak and θ is the Bragg's angle of diffraction for the peak. The relative abundance of anatase to rutile was calculated from the equation:

$$X_R = 1.26 I_R / (I_A + 1.26 I_R)$$
 (5)

Table 1: Weight fractions and crystallite size of the acid sol

	Crystal size (nm)	Crystal size (nm)	$I_{\mathbb{A}}$	I_R		
Temperature (°C)	(A)	(B)	(101)	(110)	$X_{\mathbb{A}}$	X _R
300	21.9	-	550	0	1	-
500	34.7	-	4400	0	1	-
700	53.1	67.2	5500	1600	0.73	0.27

Table 2: Weight fractions and crystallite size of the neutral sol

	Crystal size (nm)	Crystal size (nm)	I_A	I_R		
Temperature (°C)	(A)	(B)	(101)	(110)	$X_{\mathbb{A}}$	X _R
300	15.9	-	860	0	1	-
500	26.1	-	2350	0	1	-
700	45.2	41.2	3450	630	0.85	0.15

Table 3: Weight fractions and crystallite size of the base sol

	Crystal size (nm)	Crystal size (nm)	$I_{\mathbb{A}}$	I_R		
Temperature (°C)	(A)	(B)	(101)	(110)	$X_{\mathbb{A}}$	X _R
300	-	-	0	0	-	-
500	28.8	-	1300	0	1	-
700	22.3	-	820	0	1	-

where, I_R and I_A are the strongest intensities of rutile (110) and anatase (101) peaks, respectively (Su *et al.*, 2004). The average crystal sizes of TiO_2 after calcination at various temperatures are listed in Table 1-3. It is apparent that the heat treatment greatly affects the structure and the size of the resulting TiO_2 crystal. The crystal sizes for anatase increased with increasing calcination temperature, indicating aggregation of TiO_2 nanoparticles upon annealing. The fraction of rutile appears for acid and neutral sol at calcination temperature of 700°C, which is consistent that increasing the temperature of heat treatment accelerates phase transformation from thermodynamically metastable anatase to most stable and more condense rutile phase. The hydrous gel contains minute-sized TiO_2 crystal with hydroxyl groups (-OH) on the surface. During the heat treatment, the dehydration occurs and so the crystals grow to a size larger than those of the original particles.

CONCLUSION

In conclusion, the preparation of thin film ${\rm TiO_2}$ from sol gel process and tetraethyl orthotitanate precursor at different pH shows that the different pH have significant effect in the morphology, adhesion, grain size and crystallite size of the film. The SEM confirms agglomeration and increase in grain size from the prepared acid sol to base sols. While the XRD shows anatase phase to be the predominantly metastable phase at 300 to 500°C with increased crystallite size which can provide better surface area for photocatalysis. The rutile phase only appears at $700^{\circ}{\rm C}$ for the acid and neutral sol. The base sol was also observed to be the only exception because at all three temperatures the rutile phase transformation was suppressed and subsequently the intensities of the only present phase which is the anatase reduced with increasing temperature this might be as result of sodium present in the film.

ACKNOWLEDGMENT

This study was supported by Institute of Post Graduate Studies (IPS) student fellowship through School of Materials and Mineral Resources Engineering, Universiti Sains Malaysia.

REFERENCES

- Adachi, M., Y. Murata, I. Okada and S. Yoshikawa, 2003. Formation of titania nanotubes and applications for dye-sensitized solar cells. J. Electrochem. Soc., 150: 488-493.
- Anderson, C. and A.J. Bard, 1995. Improved photocatalyst of TiO₂/SiO₂ prepared by a sol-gel synthesis. J. Phys. Chem., 99: 9882-9885.
- Arconada, N., A. Durán, S. Suárez, R. Portela, J.M. Coronado, B. Sánchez and Y. Castro, 2009. Synthesis and photocatalytic properties of dense and porous TiO₂-anatase thin films prepared by sol-gel. Applied Catalysis B: Environ., 86: 1-7.
- Aruna, S.T., S. Tirosh and A. Zaban, 2000. Nanosize rutile titania particle synthesis via a ydrothermal method without mineralizers. J. Mater. Chem., 10: 2388-2391.
- Asahi, R., Y. Taga, W. Mannstadt and A.J. Freeman, 2000. Electronic and optical properties of anatase TiO₂. Phys. Rev., 61: 7459-7465.
- Asahi, R., T. Morikawa, T. Ohwaki, K. Aoki and Y. Taga, 2001. Visible-light photocatalysis in nitrogen-doped titanium oxides. Science, 293: 269-271.
- Cernigoj, U., U.L. Stangar, P. Trebse, U.O. Krasovec and S. Gross, 2006. Photocatalytically active Thin. Solid Film, 495: 327-332.
- Diez, M.A.D., A.M. Garcia, G. Silvero, R. Gordillo and R. Caruso, 2003. Theoretical study of the molecular structure for zirconium complexes. Ceram. Int., 29: 471-475.
- Fujishima, A. and K. Honda, 1972. Electrochemical photolysis of water at a semiconductor electrode. Nature, 238: 37-38.
- Fujishima, A., T.N. Rao and D.A. Tryk, 2000. Titanium dioxide photocatalysis. J. Photochem. Photobiol. C: Photochem. Rev., 1: 1-21.
- Lal, M., V. Chhabra, P. Ayyub and A. Maitra, 1998. Preparation and characterization of ultrafine TiO₂ particles in reverse micelles by hydrolysis of titanium di-ethylhexyl sulfosuccinate. J. Mater. Res., 13: 1249-1254.
- Li, Y., T. J. White and S.H. Lim, 2004. Low-temperature synthesis and microstructural control of titania nano-particles. J. Solid State Chem., 177: 1372-1381.
- Mark, H.F., D.F. Othmer, C.G. Overberger and G.T. Seaborg, 1983. Encyclopedia of Chemical Technology. 3rd Edn., John Wiley and Sons, New York, pp. 139-145.
- Miao, L., S. Tanemura, S. Toh, K. Kaneko and M. Tanemura, 2004. Fabrication, characterization and raman study of anatase-TiO₂. nanorods by a heating sol-gel template process. J. Cryst. Growth, 264: 246-252.
- Oh, S.H., R.R. Finones, C. Daraio, L.H. Chen and S. Jin, 2005. Growth of nano-scale hydroxyapatite using chemically treated titanium oxide nanotubes. Biomaterials, 26: 4938-4943.
- Scolan, E. and C. Sanchez, 1998. Synthesis and characterization of surface protected nanocrystalline titania particles. Chem. Mater., 10: 3217-3223.
- Sonawane, R.S., S.G. Hegde and M.K. Dongare, 2003. Preparation of titanium (IV) oxide thin film Mater. Chem. Phys., 77: 744-750.
- Su, C., B.Y. Hong and C.M. Tseng, 2004. Sol-gel preparation and photocatalysis of titanium dioxide. Catalysis Today, 96: 119-126.
- Sugimoto, T., X. Zhou and A. Muramatsu, 2003. Synthesis of uniform anatase TiO₂ nanoparticles by the gel-sol method 4. shape control. J. Colloid Interface Sci., 259: 53-61.
- Sugiyama, M., H. Okazaki and S. Koda, 2002. Size and shape transformation of TiO₂ nanoparticles by irradiation of 308-nm laser beam. Jap. J. Applied Phys., 41: 4666-4674.
- Sun, J. and L. Gao, 2002. pH effect on titania-phase transformation of precipitates from titanium tetrachloride solutions. J. Am. Ceram. Soc., 85: 2382-2384.

- Wu, M., G. Lin, D. Chen, G. Wang, D. He, S. Feng and R. Xu, 2002. Sol hydrothermal synthesis and hydrothermally structural evolution of nanocrystal titanium dioxide. Chem. Mater., 14: 1974-1980.
- Yin, H., Y. Wada, T. Kitamura, S. Kambe and S. Murasawa *et al.*, 2001. Hydrothermal synthesis of nanosized anatase and rutile TiO₂ using amorphous phase TiO₂ Mater. Chem., 11: 1694-1703.
- Yin, H., Y. Wada, T. Kitamura, T. Sumida, Y. Hasegawa and S. Yanagida, 2002. Novel synthesis of phase-pure nano-particulate anatase and rutile TiO₂ using TiCl₄ aqueous solutions. J. Mater. Chem., 12: 378-383.
- Zhang, W., S. Chen, S. Yu and Y. Yin, 2007. Experimental and theoretical investigation of the pH effect on the titania phase transformation during the sol-gel process. J. Cryst. Growth, 308: 122-129.